Construction and Building Materials 349 (2022) 128710

Contents lists available at ScienceDirect

Construction and Building Materials

journal homepage: www.elsevier.com/locate/conbuildmat

Bendable concrete in construction: Material selection case studies

Daiki Shoji [a,*], Bridget Ogwezi [b], Victor C. Li [a]

[a] Department of Civil and Environmental Engineering, University of Michigan, Ann Arbor, MI 48109-2125, USA
[b] Ansys, Inc., Cambridge, UK

ARTICLE INFO

Keywords:
Material selection
Engineered cementitious composites
Bridge deck link slab
Production cost
Embodied carbon footprint

ABSTRACT

Engineered cementitious composites (ECCs) have been developed to solve one of the most fundamental drawbacks in the most produced materials for our built environment. Namely, the brittle nature of concrete. ECC or 'bendable' concrete has evolved from the endeavors of a single research group to a material family in its own right, studied in hundreds of research laboratories and actively deployed in structures around the world. ECCs are a class of cementitious materials with unique tensile properties that are distinct from normal cement-based materials. This sort of material innovation is exactly what is anticipated when material property charts (Ashby charts) display empty areas in the material-property space. This paper demonstrates the uniqueness and advantages of these materials with a set of material selection case studies dealing with a bridge deck link slab. The material selection is carried out using Ansys Granta Selector, with ECCs added as new records into the existing database. The case studies show how ECCs outperform conventional concrete materials and highlight the potential of ECCs in construction.

1. Introduction

1.1. Engineered cementitious composites (ECCs)

This paper places a specific emphasis on a ceramic material technically called Engineered Cementitious Composites (ECCs). ECC is also known as "Bendable Concrete" due to its ability to undergo large flexural deflection without fracture.

ECCs belong to a class of fiber-reinforced cementitious materials that possess unique tensile properties with multiple fine cracks with the crack width of less than 100 μm, in contrast to a single large crack in concrete. ECCs are designed on the basis of micromechanics theory that enables synergistic interactions between composite components (i.e., fiber, matrix, and fiber/matrix interfaces) at the microscale [1]. High ultimate tensile strength (e.g., 10–20 MPa) typically follows. While ECCs can be tailored to also have high compressive strength (e.g., 150–200 MPa) [2], the most important and unique property of ECC, however, is its high tensile ductility, amounting to several hundred times that of normal concrete, or several % strain in tension.

The intrinsically tight crack width of ECC lends itself to significantly enhancing the tensile durability of infrastructures, including a reduction in water permeability, chloride ion diffusion, sulfate attack and other exposures typically experienced by civil infrastructure [1].

ECCs have broad and successful field applications for, but not limited to, building [3–6], transportation [6–8], and water [5,6,9] infrastructures.

Among cement-based construction materials, classification based on tensile properties has not been conventionally considered because of their intrinsic low tensile deformation capability. ECCs, therefore, represent a new category of cement-based materials.

1.2. Granta Selector

Ansys Granta Selector features a comprehensive database, storing engineering, economic, and environmental properties for more than 4,000 materials [10,11]. Furthermore, any new material records can be supplemented, as necessary, by manually inputting the records. This attribute allows users to assess any likelihood of the newly added materials to be substituted for originally stored ones, while comparing them for better material selections.

With this functionality in Granta Selector, a dataset for various types of ECCs was newly created and manually installed in Granta Selector's material library. The database was built by a preliminary literature review performed by the authors, which is available in the supplementary information file. The ECCs in this database are categorized into 13 different types, at the time of writing this paper, based on their intended

* Corresponding author.
E-mail addresses: daikinsh@umich.edu (D. Shoji), bridget.ogwezi@ansys.com (B. Ogwezi), vcli@umich.edu (V.C. Li).

https://doi.org/10.1016/j.conbuildmat.2022.128710
Received 15 March 2022; Received in revised form 22 June 2022; Accepted 4 August 2022

functions. Examples include high-strength ECC, lightweight ECC, high-ductile ECC, and green (i.e., environmentally friendly) ECC. The categorized, function-based ECCs have multiple mix designs amounting to 47 in total. Each mix design contains as many properties as can be obtained from published papers and articles (Fig. 1). Because most of these datasets are from research publications, their property range may be large due to variability in test data. Granta Selector currently does not have the property of tensile ductility or tensile strain capacity for cementitious materials. For this reason, the existing property "Elongation" is used to represent the tensile ductility or tensile strain capacity of ECC.

The unique features of ECC when compared to other common cementitious materials are illustrated in Figs. 2 and 3. Fig. 2 shows a plot of the tensile strength and ductility of ECC groups mentioned above. The tensile strength ranges from about 1 MPa for fire-resistive sprayable ECC to about 20 MPa for high-strength high ductility ECC. The tensile strain capacity ranges from about 1 % to 10 %. Most of the normal cementitious materials lie on the lower left corner of this plot. The only member in this family that shows high tensile strength (about 10 MPa) is high-performance concrete and that shows high tensile strain capacity (about 1 %) is asphalt concrete. A variety of ECCs tend to combine these two properties.

Fig. 3 shows a plot of the compressive strength against tensile ductility for ECCs and some common concrete materials in the standard Granta Selector database. As shown, the compressive strength of high-strength ECC can reach over 100 MPa while maintaining high tensile ductility close to 10 %.

Figs. 2 and 3 shows that ECC fills the empty space on the upper right-hand corner of these Ashby charts, following the development vector for cementitious materials with high strength and tensile ductility. The distinction of ECCs, when it comes to the material selection for infrastructure design, is illustrated in three practical examples detailed in the next section.

2. Bridge deck link slab: Material selection case studies

In this section, a set of three realistic examples is established to explain the process of material selections [12,13] dealing with a bridge deck link slab jointed between adjacent concrete slabs. The concrete slabs connected with a link slab behave in a continuous manner, while the steel girders under the deck remain simply supported. This kind of joint system eliminates negative impacts caused by mechanical expansion joints conventionally placed over piers and abutments of multispan bridges. Debris accumulation and water/salts leakage in and through the joints promote early malfunction of the mechanical joints themselves and bridge girder bearings or supporting structures, respectively [14]. This entails frequent maintenance and repair work, which is costly for the individual state departments of transportation [15]. The link slabs thus aim at replacing the mechanical expansion joints so that a smooth and continuous deck surface can be constructed, and thereby addressing such negative problems [8]. Research and field-scale applications using the link slab have been implemented [16,17]. The visual context of the examples is illustrated in Fig. 4. The essential function of the link slab is to accommodate uniaxial expansion and contraction of the steel girders that sits on roller supports as shown. The concrete bridge deck is coupled to the girders via shear studs. The design aims at concentrating much of the deformation in the link slab as well as minimizing deformation (especially tensile) and avoiding crack formation in the concrete bridge deck.

2.1. Single objective problem 1: minimizing cost

Translation of design requirements: The first step to be taken is to translate the design or application requirements into constraints and objectives. The constraints are to be guaranteed (i.e., must-haves), while the objectives are to be accomplished (i.e., nice-to-haves) by definition. In this example, a few constraints include, but not limited to, that; the desired link slab must be cast-in-place and its sectional geometry (i.e., t_s and b) must be identical to that of adjacent concrete slabs, for instance (Table 1). The most critical constraint, among them, is that the link slab must possess a good tensile strain capacity [14]. This is so identified by asking what would cause the link slab to lose its functionality. In this case, excessive girder expansion/contraction ΔL_g induced by fluctuating temperature would likely devastate the link slab in service. The link slab therefore must possess deformability ΔL_l (over its length L_l unbonded to the girder) enough to accommodate such a deformation demand ΔL_g from the girder without experiencing tensile fracture. The derivation process is shown below, using the definition of thermal coefficient α [unit: 1/°C] shown in Eq. (1):

$$\alpha = \frac{\Delta L_g}{L_g}\frac{1}{\Delta T}, \tag{1}$$

where ΔL_g is the extra girder deformation (i.e., demand), L_g is the girder length, and ΔT is the maximum temperature difference [°C] in temperature cycles. Since the link slab is to accommodate the demand ΔL_g, its deformation capacity ΔL_l (i.e., supply) must be greater than ΔL_g, formulating a constraint function below:

$$\begin{aligned} \Delta L_l &> \Delta L_g \\ L_l\varepsilon_l &> \alpha L_g \Delta T \\ L_l &> \frac{\alpha L_g \Delta T}{\varepsilon_l}, \end{aligned} \tag{2}$$

where L_l is the link slab length and ε_l is the uniaxial strain capacity of

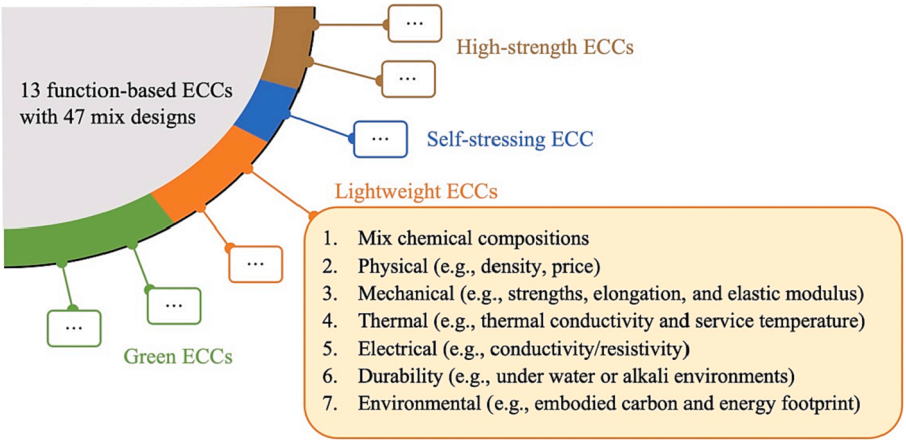

Fig. 1. Schematic diagram of the ECC database in Granta Selector.

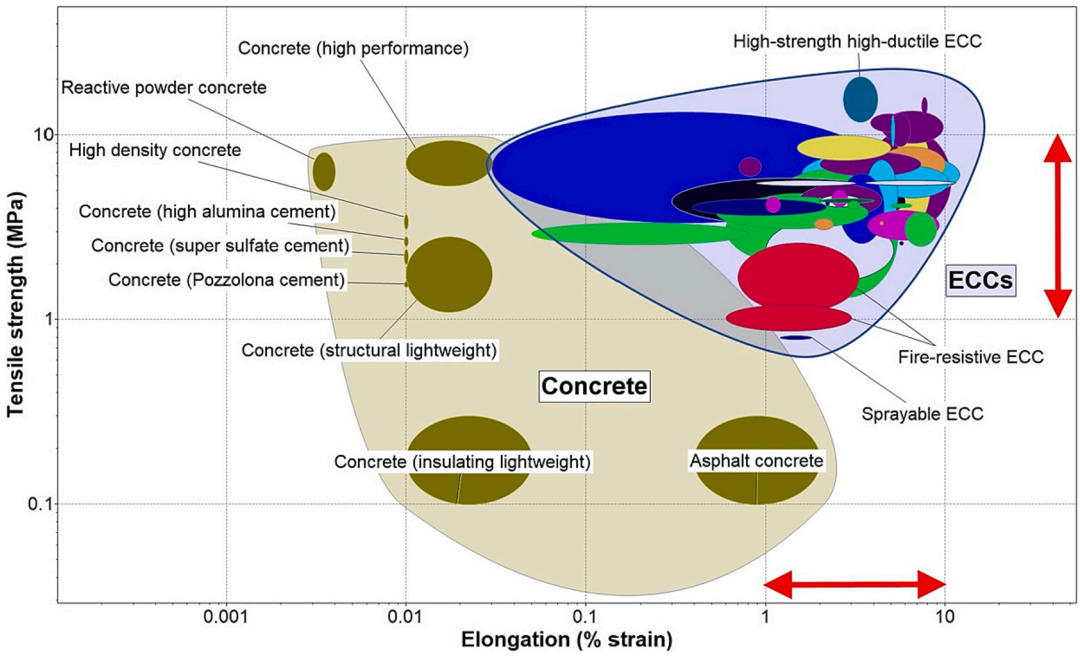

Fig. 2. Bubble chart of tensile strength and tensile ductility of ECCs and common concrete materials in Granta Selector. The two large bubbles in lighter color represent the family of concrete and the family of ECCs.

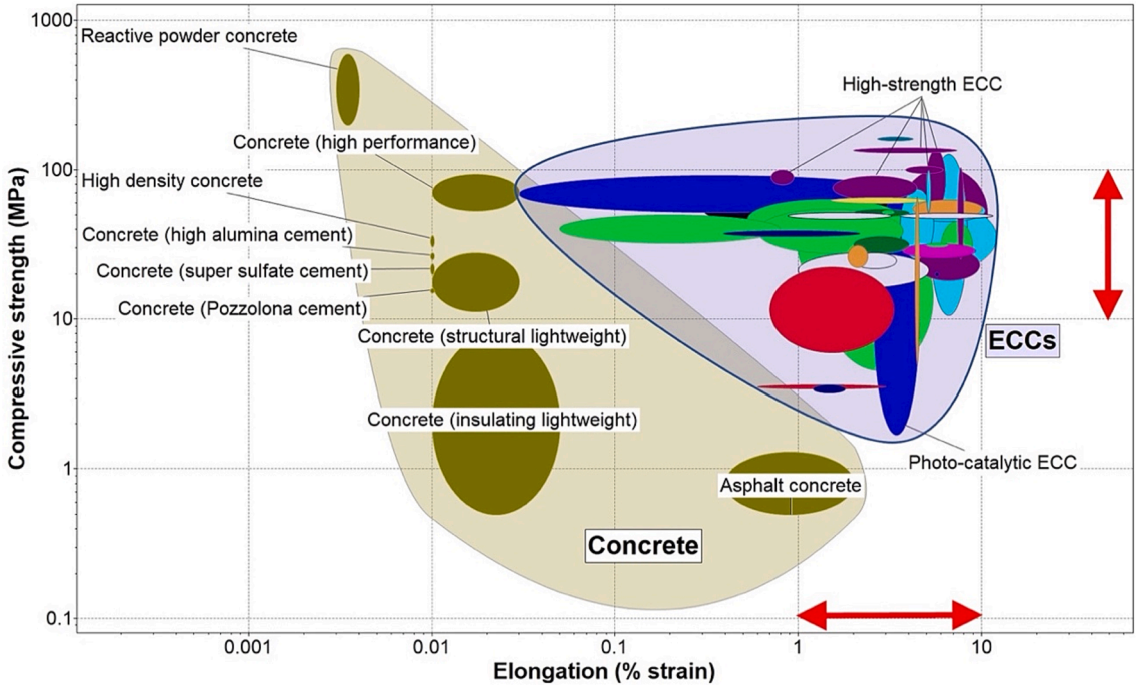

Fig. 3. Bubble chart of compressive strength and tensile ductility of ECCs and common concrete materials in Granta Selector.

the link slab. This constraint function suggests that any material with good strain capacity can allow for the link slab shortened. It should be also noted here that how strong the link slab is not as important as how deformable it is. Indeed, flexural flexibility of the link slab is preferred to maintain the original simply-supported beam-end design of the bridge deck. While taking care of those constraints above, we set an objective of minimizing the cost associated with material production alone. The first step is summarized in Table 1.

Objective function: The objective of minimizing the cost of the link slab can be expressed as

$$\begin{aligned} \text{Min Cost} &= C_m \cdot \rho V \\ &= C_m \cdot \rho (b t_s L_l), \end{aligned} \tag{3}$$

where C_m: cost per unit mass [cost (USD)/kg], ρ: density [kg/m^3], V: volume of the link slab [m^3], b: slab width [m], t_s: slab thickness [m], L_l: link slab length [m].

Material index: The material index can be derived by combining Eqs. (2) and (3). Thus,

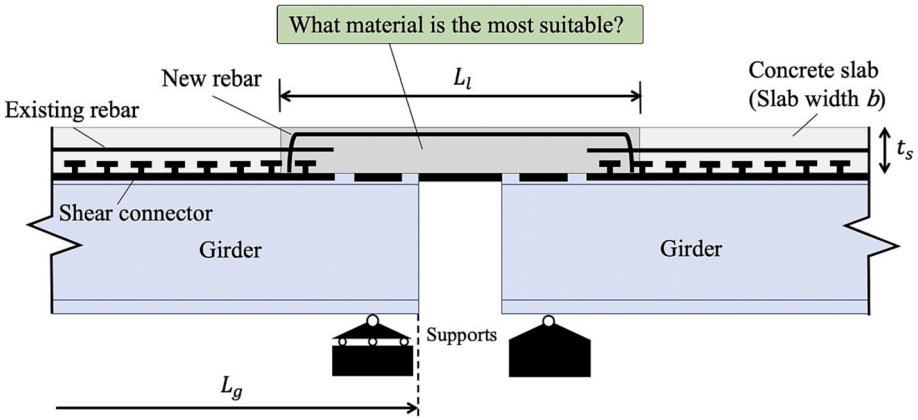

Fig. 4. Illustration of a bridge deck link slab [8] for which material selection examples are performed.

Table 1
Design requirements for the link slab.

Function	Bridge deck link slab to serve the function of a conventional expansion joint
Constraints	• Must be able to be cast on site • Thickness t_s and width b to match those of concrete deck • Must have stiffness similar to or less than that of adjacent concrete deck • Must be durable for traffic loads • Service temperature for southern MI • Must accommodate temperature-induced expansion and contraction ($\Delta L_l > \Delta L_g$)
Objectives	Minimize cost (of the bridge deck link slab)
Free variables	• Length of the link slab L_l • Choice of material

$$\begin{aligned} \text{Min Cost} &= C_m{\cdot}\rho(bt_sL_l) \\ &> C_m{\cdot}\rho\left(bt_s\frac{\alpha L_g\Delta T}{\varepsilon_l}\right) \\ &> bt_s{\cdot}\alpha L_g{\cdot}\Delta T{\cdot}\left(\frac{\rho C_m}{\varepsilon_l}\right) \end{aligned}$$

implies minimizing $\left(\frac{\rho C_m}{\varepsilon_l}\right)$ or maximizing the material index $M_1 = \left(\frac{\varepsilon_l}{\rho C_m}\right)$.

The first term bt_s on the right-hand side of this inequality above accounts for the geometric parameters of the bridge deck, while the second αL_g involves parameters associated with the steel girder. The third term ΔT represents the driving force behind the thermal deformation and is linked to the diurnal temperature cycle of the location where the bridge is located. Each of them is either a fixed or already specified in the design. The fourth term $\left(\frac{\rho C_m}{\varepsilon_l}\right)$ involves a combination of three material parameters dependent on the choice of material. The other free variable in this optimization problem is the length of the link slab L_l.

Material screening: Following the identification of the material index M_1, the next step is called material screening. This is performed by

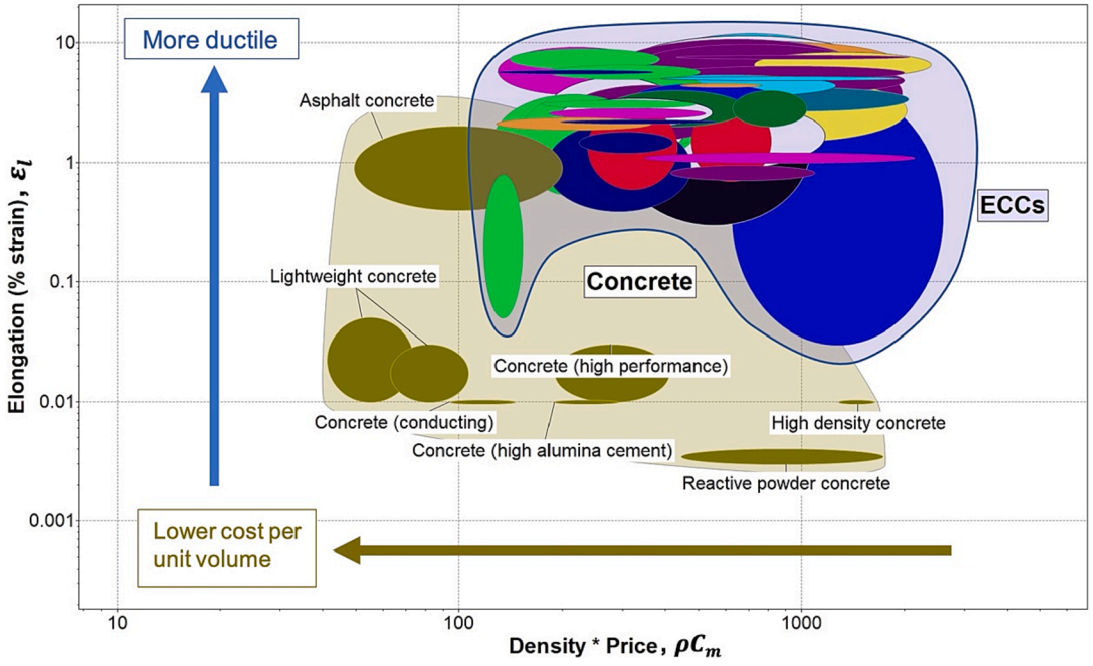

Fig. 5. Elongation (i.e., tensile strain capacity) plotted against price per volume of concrete and ECCs.

applying the constraints found in the first step. For instance, the on-site castability of desired materials eliminates majority of materials including the family of metals. The groups of metals are also excluded by the requirement that the link slab must have a stiffness similar to or less than that of the adjacent concrete slabs. Durability concerns including UV resistance, wear resistance from traffic load, and slippery surface for automobile braking eliminate the family of polymers. Those constraints screen out most materials and reduce the number of viable materials to two candidates: the group of concrete and ECC materials (Fig. 5).

Material ranking: The material screening helps isolate materials capable of doing the required job. The material ranking, as its name suggests, orders the candidates that can perform best based on the material index, M_1. Being plotted on a material property chart with the logarithmic scales for both axes as shown in Fig. 6, the material index line is moved upper left to maximize M_1 such that a few optimal materials can be located. Fig. 7 then identifies the materials with higher values of M_1. The concrete materials (e.g., lightweight concrete and high-performance concrete) generally perform better as far as the cost alone is concerned; however, they become out of consideration due the lower values of M_1 resulting from their inherent low tensile capacity (see also Fig. 5). It should also be noted that asphalt concrete originally stored in Granta Selector could possibly be used for the link. It is ranked 5th when various higher ranking ECCs are considered.

Documentation: After the material ranking, the free variables (i.e., the choice of material and length of the link slab) and objective (i.e., minimized cost) are investigated according to M_1. Table 2 summarizes this assessment for some of the most promising materials. Asphalt concrete is included for the sake of comparison. Sprayable ECC (FA/LC3/CSA-PP), ranked third in M_1 value, is eliminated because its sprayable nature does not fit the cast-in-place process requirement for the link slab application. The cost per unit volume of the asphalt concrete is much less than that of the ECCs, as previously shown in Fig. 5. That being said, the table shows a distinction between the group of viable ECCs and asphalt concrete. The link slab could be shortened, and the material production cost accordingly reduced by adopting the family of ECCs. The better tensile performance of the ECCs over the asphalt concrete gives rise to saving the amount of material for the link slab, thus lowering the link-slab production cost. The calculation of the minimal length and minimal production cost of the link slab is based on the following assumed quantities [1,18,19]: steel girder length $L_g = 60$ [m]; thermal expansion coefficient $\alpha = 12\mu$ [1/°C]; slab thickness $t_s = 225$ [mm]; slab width $b = 20.25$ [m]; and temperature difference $\Delta T = 20$ [°C].

2.2. Single objective problem 2: minimizing carbon footprint

Translation of design requirements: Here, another objective of minimizing carbon footprint associated with material production is discussed. This is because of the growing concern over sustainability in the cement and concrete industry [20]. The translation of the design requirements is identical to the first example as shown in Table 1, except for the new objective.

Material index: Following the same procedure, the material index M_2 for this problem is derived as.

$$\text{Material index } M_2 = \frac{\varepsilon_l}{\rho CO_2} \text{(to be maximized)},$$

where CO_2 is the embodied carbon per unit material mass [kg CO_2/kg].

Material screening: The same reasoning as for the first example is applied to screen out materials not satisfying any of the constraints, leaving concrete and ECCs to be ranked in the next step.

Material ranking: The way of interpreting Fig. 8, which plots the tensile strain capacity against the carbon footprint on a unit volume basis, is analogous to that in Fig. 7. Fig. 8 shows that, when the minimized carbon footprint is favored, the optimal choice differs from that for minimized cost. It should be noted here that the asphalt concrete, which was ranked 5th for the minimized cost, now becomes a much less plausible candidate due to its high embodied carbon and lower tensile strain capacity, while some additional ECCs become better solutions

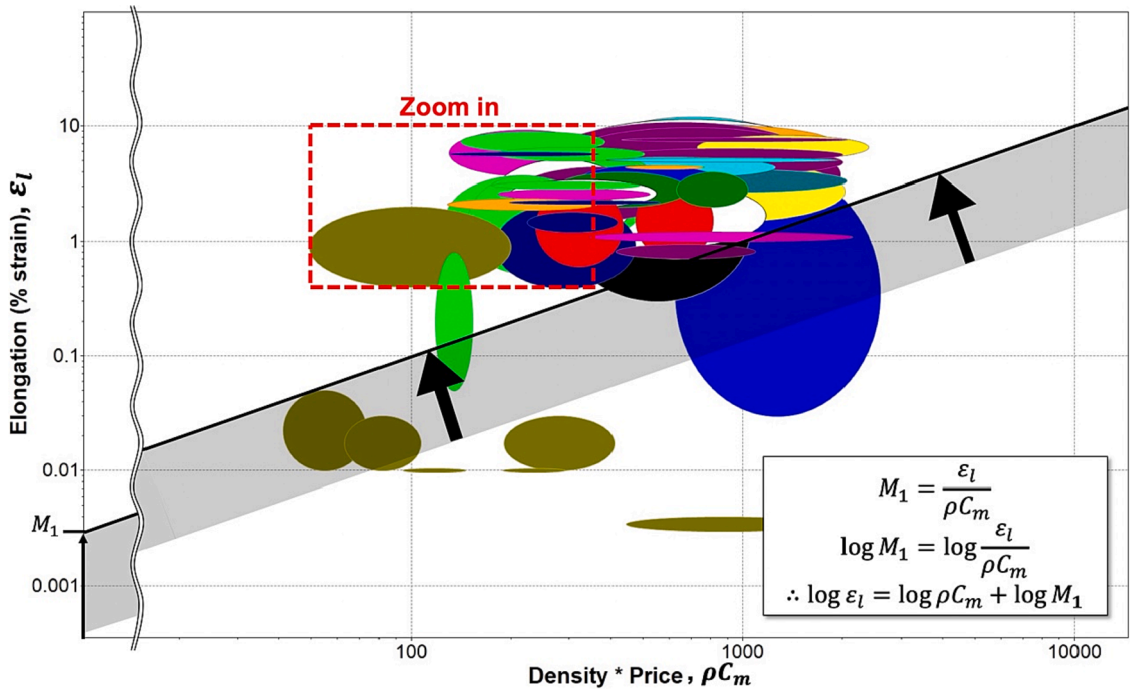

Fig. 6. Material ranking for the link slab whose objective is minimize the production cost of the link slab. The material index M_1 is defined such that the objective is accomplished by maximizing M_1. Moving the material index line (a straight line with slope of unity), which is shown black in this material property chart, to the upper left narrows down the options of preferred materials. This graphical procedure accordingly maximizes the material index M_1 whose value corresponds to the intercept on the vertical axis.

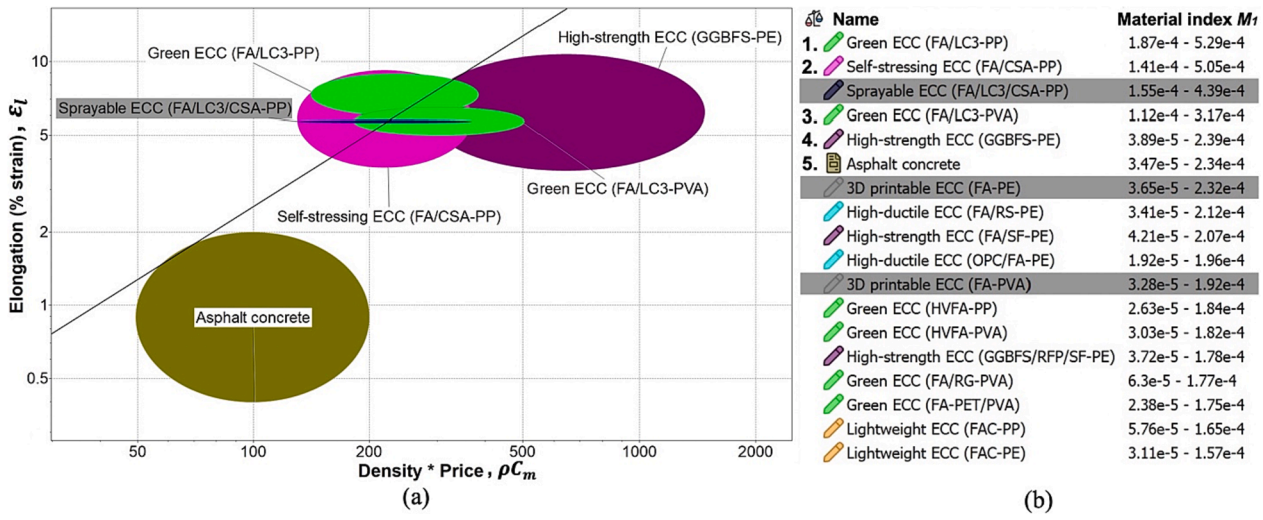

Fig. 7. (a) Zoom-in portion of Fig. 6 retaining only materials with higher M_1 values (b) Material ranking for the link slab with the objective of minimizing the cost. Possible candidates are listed in descending order based on their M_1 values. Asphalt concrete, which is originally stored in Granta Selector is now ranked 5th. Sprayable ECC (FA/LC3/CSA-PP), however, is excluded by imposing a processing requirement.

Table 2
Selection of a material for the link slab minimizing the production cost.

Material	M_1 [a]	Min.L_l	Min. Cost
	[m^3/USD]	[m]	[USD]
Green ECC (FA/LC3-PP[b])	3.58×10^{-4}	0.19	183
Self-stressing ECC (FA/CSA-PP[c])	3.23×10^{-4}	0.22	203
Green ECC (FA/LC3-PVA[d])	2.15×10^{-4}	0.25	306
Asphalt concrete	1.34×10^{-4}	1.20	488

[a] Mean value of the M_1 range shown in Fig. 7(b).
[b] Fly ash (FA), limestone calcined clay cement (LC3), and polypropylene (PP) fiber are included as main ingredients.
[c] Calcium sulfoaluminate (CSA) cement is included besides FA and PP fiber.
[d] Polyvinyl alcohol (PVA) fiber is included as well as FA and LC3.

with higher M_2 values.

Documentation: Table 3 shows the comparison of M_2, minimal L_l, and minimal carbon footprint for the link slab for a few top-ranked materials plus the asphalt concrete. Analogous to the first example, the on-site casting processing requirement eliminates 3D-printable ECC (FA-PE). High-ductile ECC (FA/RS-PE), which is ranked first in Fig. 8 (b) becomes the second choice if a mean value of M_2 is taken into account. This means that this kind of ECC has a relatively large range of the M_2 value, compared to Green ECC (FA/LC3-PP). The asphalt concrete, which was ranked 5th in the first example, is now ranked 14th. As Fig. 9 shows, the family of ECCs as a whole tend to emit higher CO_2 than concrete materials on a unit volume basis due to higher cement content and the use of synthetic fibers. However, similar to the cost problem, the adoption of technically superior ECCs allows much less volume of materials needed for the link slab than the asphalt concrete, thereby reducing the considerable amount of the carbon dioxide emission of the designed link slab.

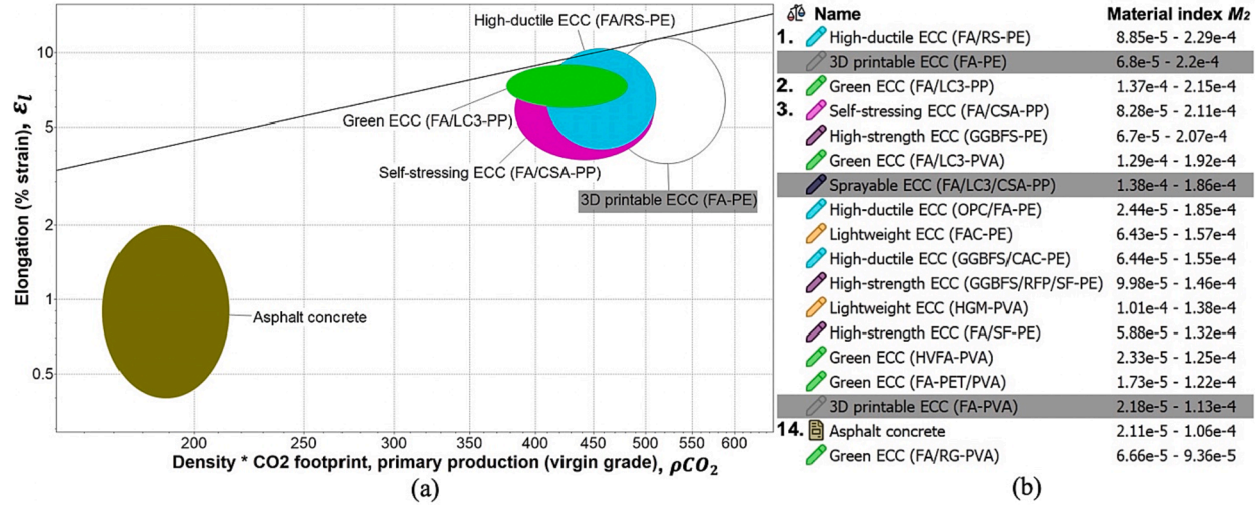

Fig. 8. Material ranking for the link slab with the objective of minimizing the carbon footprint. (a) The viable materials are ranked differently from the case of minimizing cost (a portion of Fig. 9). (b) The asphalt concrete, which was ranked 5th in the first example, is now ranked 14th, becoming a less viable material.

Table 3
Selection of a material for the link slab minimizing the carbon footprint.

Material	M_2[a]	Min.L_l	Min. carbon footprint
	[m^3/ kg CO_2]	[m]	[kg CO_2]
High-ductile ECC (FA/RS-PE[b])	1.59×10^{-4}	0.20	413
Green ECC (FA/LC3-PP[c])	1.76×10^{-4}	0.19	373
Self-stressing ECC (FA/CSA-PP[d])	1.47×10^{-4}	0.22	447
Asphalt concrete	0.63×10^{-4}	1.20	1032

[a] Mean value of the M_2 range shown in Fig. 8(b).
[b] Fly ash (FA), river sand (RS), and polyethylene (PE) fiber are included as primary ingredients.
[c] Limestone calcined clay cement (LC3) and polypropylene (PP) fiber, in addition to FA, are included.
[d] Calcium sulfoaluminate (CSA) cement is blended as well as FA and PP fiber.

2.3. Multiple objectives problem: cost vs carbon footprint

The previous two examples dealt with a single objective each, for simplicity; however, real-life material selections entail more to consider. In reality, at least four objectives would be ideally considered as follows: minimizing (a) mass, (b) volume, (c) cost, and (d) environmental impact [12]. That said, they typically conflict each other and need to be optimized in a way that a compromise can be reached between those conflicting objectives.

One way to deal with multiple objectives simultaneously is to use a penalty function Z [12]. The penalty function is formulated with as many objectives (i.e., material indices) as desired. The most preferable solution is defined as the value of Z minimized after converting various objective units into a single unit with multiplication of exchange constants. This last example shall discuss a multi-objectives problem of minimizing both carbon footprint and cost. The penalty function Z for this example is then formulated as.

$$Z = M_1' + \beta M_2' = \left(\frac{\rho C_m}{\varepsilon_l}\right) + \beta\left(\frac{\rho CO_2}{\varepsilon_l}\right) = \frac{\rho}{\varepsilon_l}(C_m + \beta CO_2),$$

where Z: penalty function [USD], M_1', M_2': the material indices to be minimized, β: exchange constant [USD/kg CO_2]. The β-value can be considered a carbon tax; it converts unit reduction of carbon in kg to dollar cost.

Figs. 10 and 11 show results of material ranking for two possible scenarios: in case we place an emphasis on the carbon footprint rather than the cost, and vice versa. Such a consideration is enabled by taking different values for the exchange constant, β.

For β equal to 10, the carbon footprint is of prime importance because the price due to one increment of carbon footprint is increased tenfold, becoming much more influential in the final quantity of the penalty function, Z. On the contrary, the cost is prioritized over the carbon footprint if β is taken to be 0.1 since the impact of price increase associated with the carbon footprint will drop to one-tenth. In this example, real carbon tax whose extreme values equal 0.001 and 0.137 USD/kg CO_2 as of 2021 were taken into consideration [21].

For both cases, the most suitable material is found to be Green ECC (FA/LC3-PP), which includes fly ash (FA), limestone calcined clay cement (LC3), and polypropylene (PP) fiber as its primary ingredients. This is due to the convex shape of the Pareto front with interior angle about 90° enveloping the viable non-dominated material bubbles. Beyond Green ECC, the next best choices are indeed influenced by the value of β, as shown by the ranking movements indicated by the arrows in Fig. 11.

3. Summary and conclusion

The examples for the design of bridge deck link slabs show that the tensile ductility plays a key role in the material selection that initially seeks either minimized cost or carbon footprint, and ultimately both. The optimal material choices turn out to be from the ECC family with high tensile ductility, and not from any of the conventional concrete materials. Specifically, green ECC, which includes fly ash, limestone calcined clay cement, and polypropylene fiber as its primary

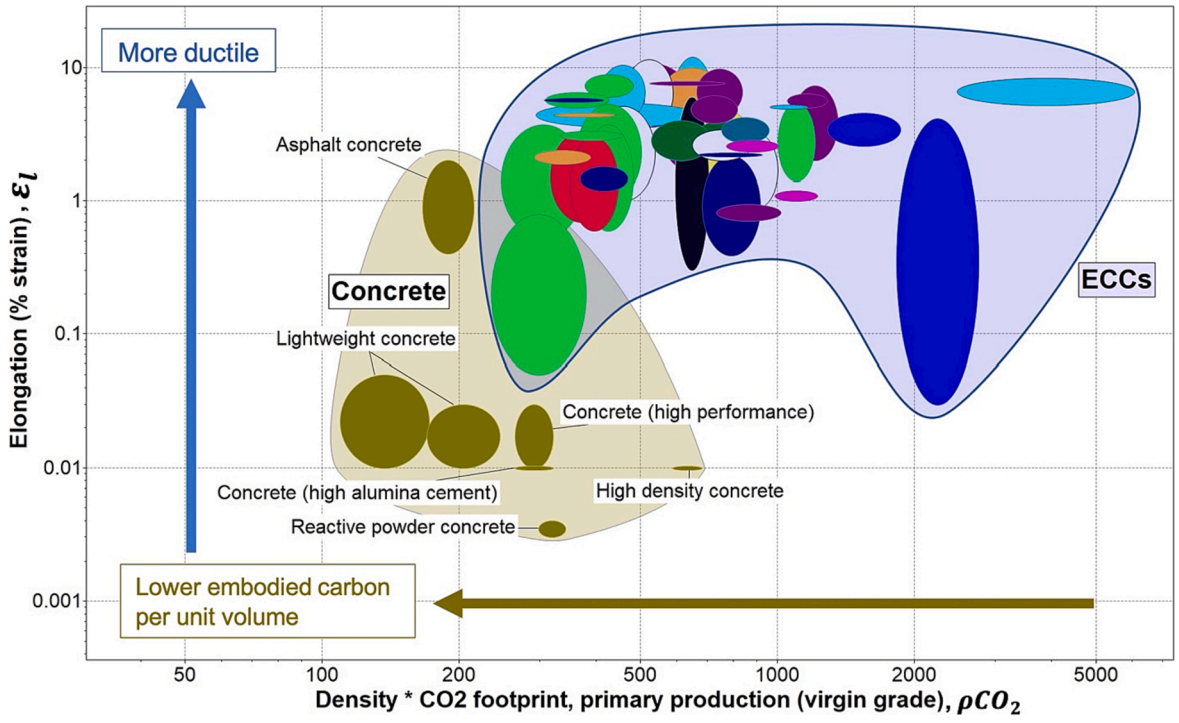

Fig. 9. Elongation plotted against embodied carbon footprint per volume of concrete and ECCs.

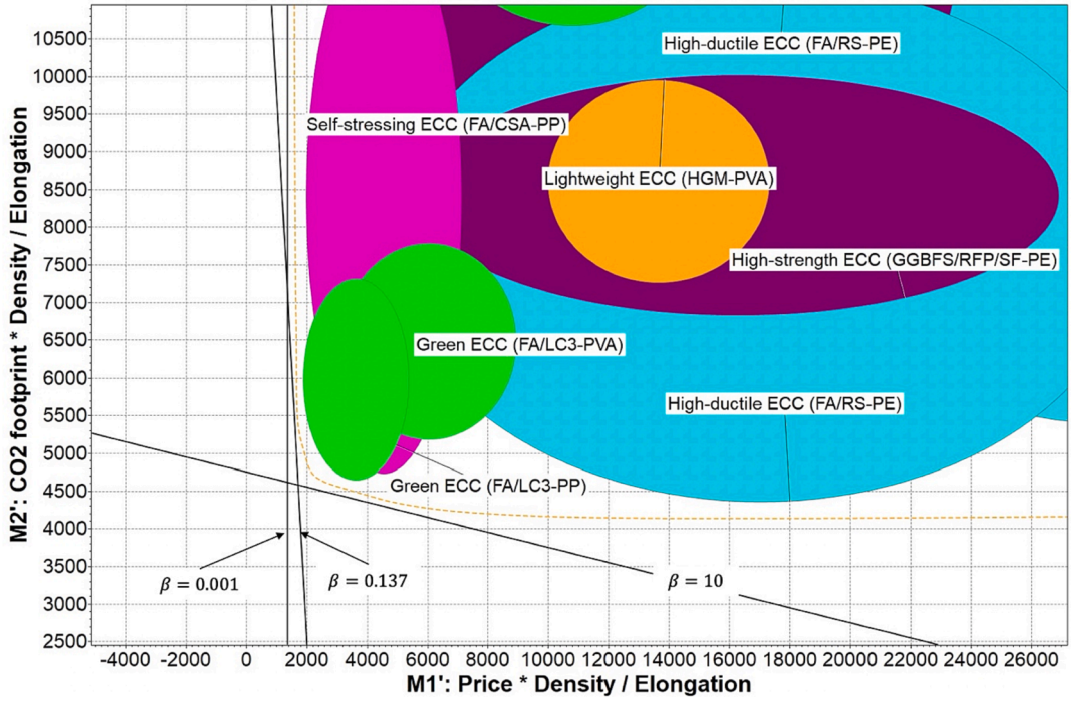

Fig. 10. The trade-off plot (on linear axis) for the multiple objective problem. The material ranking is dependent on the value of the exchange constant, β.

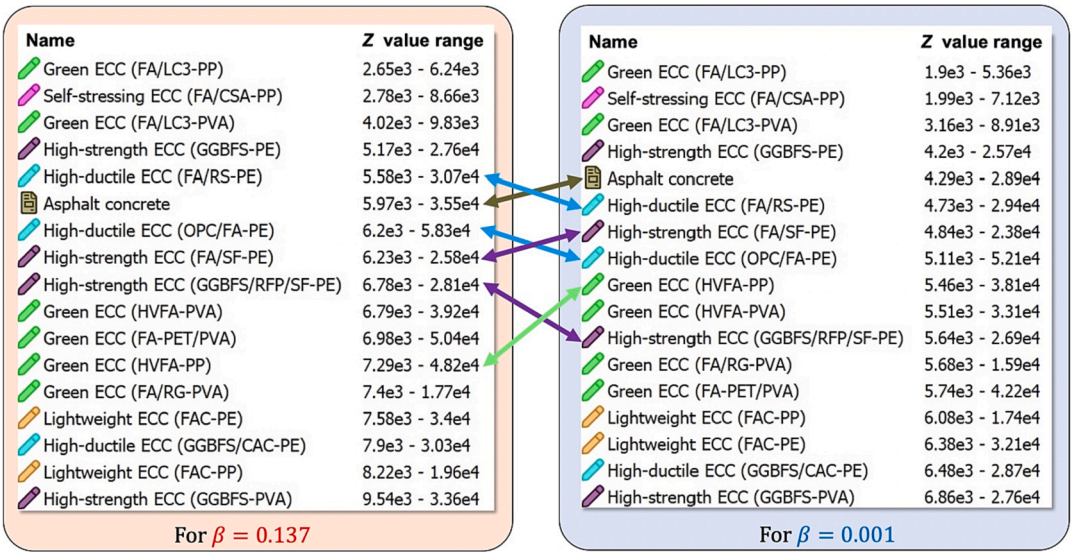

Fig. 11. Preferred material options are based on the penalty function Z to be minimized. The result varies with the two different scenarios depending on whether price or carbon footprint is to be prioritized: for $\beta = 0.137$ (left) and for $\beta = 0.001$ (right).

ingredients, is the most favorable option regardless of the magnitude of the carbon tax.

It is concluded that lower economic cost and embodied carbon bridge deck link slabs can be designed using ECC slabs of shorter length, despite ECC's higher cost and carbon intensity on a unit mass or volume basis when compared with other concrete materials.

The use phase reduction in carbon and energy footprints for ECC link slab has been established in prior studies using a comprehensive life-cycle model [22]. Together with the findings in this paper, it is demonstrated that reductions in carbon emissions for both dominating life-cycle phases of material production and infrastructure use can be achieved with the selection of green ECC. The value proposition of ECC for long term durability and operational carbon reduction is long known. This paper offers new insights into the reduction of upfront carbon emission in the design of civil infrastructure.

The family of truly ductile ECCs has expanded the limit of material properties, filling up empty areas on Ashby's charts, notably for tensile properties in brittle materials. This means that the ECCs offer new and better options in the material selection for civil infrastructure expected to experience large tensile deformation and/or potential crack-induced water leakage such as underground construction or water containing structures. The intrinsic crack-width control and self-healing ability in ECC promotes overall better durability performance during infrastructure operation. Additional incentives to select ECCs over conventional concrete materials derive from long-term benefits in economic and ecological costs associated with maintenance and repairs.

Finally and on a broader perspective, this work reveals how micromechanics, which forms the design basis of ECC, translates into economic and ecological benefits of the large scale built environment.

CRediT authorship contribution statement

Daiki Shoji: Writing – original draft, Data curation, Visualization. **Bridget Ogwezi:** Resources, Software, Writing – review & editing. **Victor C. Li:** Supervision, Writing – review & editing.

Declaration of Competing Interest

The authors declare that they have no known competing financial interests or personal relationships that could have appeared to influence the work reported in this paper.

Data availability

The created ECC database for use in Granta Selector (.ces) is available in Appendix A.

Acknowledgement

This work was conducted under the technical support of Ansys, Inc. and the University of Michigan Center for Low Carbon Built Environment (CLCBE) and did not receive any grant from funding agencies in the public, commercial, or non-profit sectors.

Appendix A. Supplementary data

Supplementary data to this article can be found online at https://doi.org/10.1016/j.conbuildmat.2022.128710.

References

[1] V.C. Li, Engineered Cementitious Composites (ECC), 1st ed., Springer, 2019. https://doi.org/10.1007/978-3-662-58438-5.
[2] K. Yu, L. Li, J. Yu, Y. Wang, J. Ye, Q.F. Xu, Direct tensile properties of engineered cementitious composites: A review, Constr. Build. Mater. 165 (2018) 346–362, https://doi.org/10.1016/J.CONBUILDMAT.2017.12.124.
[3] T. Kanda, S. Nagai, M. Maruta, Y. Yamamoto, New High-rise R/C Structure Using ECC Coupling Beams, in: R.D. Toledo Filho, F.A. Silva, E.A.B. Koenders, E.M.R. Fairbairn (Eds.), 2nd International RILEM Conference on Strain Hardening Cementitious Composites, RILEM Publications SARL, Rio de Janeiro, 2011: pp. 289–296.
[4] M. Maruta, T. Kanda, S. Nagai, Y. Yamamoto, New High-rise RC Structure Using Pre-cast ECC Coupling Beam, Concr. J. 43 (2005) 18–26, https://doi.org/10.3151/coj1975.43.11_18.
[5] K. Rokugo, T. Kanda, H. Yokota, N. Sakata, Applications and recommendations of high performance fiber reinforced cement composites with multiple fine cracking (HPFRCC) in Japan, Materials and Structures/Materiaux et Constructions (2009) 1197–1208, https://doi.org/10.1617/s11527-009-9541-8.
[6] K. Rokugo, Tension tests and structural applications of strain-hardening fiber-reinforced cementitious composites, in: 7th International Conference on Fracture Mechanics of Concrete and Concrete Structures, Korea Concrete Institute, Jeju, 2010: pp. 1533–1540.
[7] J. Zhang, Z. Wang, X. Ju, Application of ductile fiber reinforced cementitious composite in jointless concrete pavements, Compos. B Eng. 50 (2013) 224–231. https://doi.org/10.1016/j.compositesb.2013.02.007.
[8] M.D. Lepech, V.C. Li, Application of ECC for bridge deck link slabs, Materials and Structures/Materiaux et Constructions 42 (2009) 1185–1195, https://doi.org/10.1617/s11527-009-9544-5.
[9] S. Müller, V. Mechtcherine, Use of Strain-Hardening Cement-Based Composites (SHCC) in Real Scale Applications, in: V. Mechtcherine, V. Slowik, P. Kabele (Eds.), Strain-Hardening Cement-Based Composites, Springer, Netherlands, Dordrecht, 2018, pp. 690–700.
[10] Ansys Granta, Ansys Granta Selector – Materials Selection Software, (2021). https://www.ansys.com/products/materials/granta-selector (accessed November 17, 2021).
[11] Ansys Granta, Material Universe, (2021). https://www.grantadesign.com/industry/ products/data/materialuniverse (accessed November 25, 2021).
[12] M.F. Ashby, Materials Selection in Mechanical Design, Elsevier Science, 2010. https://www.elsevier.com/books/materials-selection-in-mechanical-design/ashby/978-0-08-095223-9.
[13] M.F. Ashby, Materials and the Environment: Eco-informed Material Choice, Elsevier Science, 2012. https://www.elsevier.com/books/materials-and-the-environment/ashby/978-0-12-385971-6.
[14] G. Haikal, J.A. Ramirez, M.R. Jahanshahi, S. Villamizar, O. Abdelaleim, Link Slab Details and Materials (2019), https://doi.org/10.5703/1288284316920.
[15] A. Caner, P. Zia, Behavior and design of link slabs for jointless bridge decks, PCI J. 43 (1998) 68–78. https://doi.org/10.15554/PCIJ.05011998.68.80.
[16] A. Mostafa, A. Elmanney, L.S. Radwan, A. Gadellah, Review Paper on Link Slab Bridge Girder Technique, Int. J. Eng. Res. Technol. 9 (2020).
[17] E.T. Thorkildsen, Greenman-Pedersen, Case Study: Eliminating Bridge Joints with Link Slabs – An Overview of State Practices, United States. Federal Highway Administration, 2020. https://doi.org/10.21949/1503647.
[18] M.A. Grubb, K.E. Wilson, C.D. White, W.N. Nickas, Load and Resistance Factor Design (LRFD) For Highway Bridge Superstructures – Reference Manual, 2015.
[19] National Weather Service, Climate, (2021). https://www.weather.gov/wrh/climate (accessed December 18, 2021).
[20] J. de Brito, R. Kurda, The past and future of sustainable concrete: A critical review and new strategies on cement-based materials, J. Cleaner Prod. 281 (2021), 123558, https://doi.org/10.1016/j.jclepro.2020.123558.
[21] W. Bank, State and Trends of Carbon Pricing 2021, Washington, DC, 2021. https://openknowledge.worldbank.org/handle/10986/35620.
[22] G.A. Keoleian, A. Kendall, J.E. Dettling, V.M. Smith, F. Richard, M.D. Chandler, V. C.L. Lepech, Life Cycle Modeling of Concrete Bridge Design: Comparison of Engineered Cementitious Composite Link Slabs and Conventional Steel Expansion Joints, J. Infrastruct. Syst. 11 (2005) 51–60, https://doi.org/10.1061/(ASCE)1076-0342(2005)11:1(51).